

Electronic Supplementary Information for

Tunable Photoluminescence Properties of Fluorescein in a Layered Double Hydroxide Matrix and its Application in Sensor

Wenying Shi, Min Wei,* David G. Evans, Xue Duan

*State Key Laboratory of Chemical Resource Engineering, Beijing University of Chemical Technology,
Beijing 100029, P. R. China*

CORRESPONDING AUTHOR FOOTNOTE

* Corresponding author. Phone: +86-10-64412131. Fax: +86-10-64425385. E-mail: weimin@mail.buct.edu.cn.

List of Contents:

Figure S1. Three-dimensional perspective for the experimental setup to record fluorescence spectra with linear polarized light in the front-face configuration of a PTI Fluorescence instrument. The twist angle δ of the sample with respect to the excitation beam is also illustrated.

Figure S2. The FWHM of XRD patterns for (A) Zn₂Al-NO₃-LDH and (B) FLU-HES/LDH ($x\%$): (a)~(h) $x=1.00\times10^{-3}\%$, $6.80\times10^{-3}\%$, $1.25\times10^{-2}\%$, $2.00\times10^{-2}\%$, $1.00\times10^{-1}\%$, 1.05%, 38.0% and 100%, respectively.

Figure S3. FT-IR spectra (4000~400 cm⁻¹ region) for the FLU-HES/LDH ($x\%$): (a)~(i) $x=0$, $1.00\times10^{-3}\%$, $6.80\times10^{-3}\%$, $1.25\times10^{-2}\%$, $2.00\times10^{-2}\%$, $1.00\times10^{-1}\%$, 1.05%, 38.0% and 100%, respectively.

Figure S4. Fluorescent microscopic photographs of the FLU-HES/LDH films ($x\%$): (a)~(h) $x=1.00\times10^{-3}\%$, $6.80\times10^{-3}\%$, $1.25\times10^{-2}\%$, $2.00\times10^{-2}\%$, $1.00\times10^{-1}\%$, 1.05%, 38.0% and 100%. All the samples were excited by blue light.

Figure S5. The fluorescence quantum yield varying with the increase of FLU content in the FLU-HES/LDH ($x\%$). $x=1.00\times10^{-3}\%, 6.80\times10^{-3}\%, 1.25\times10^{-2}\%, 2.00\times10^{-2}\%, 1.00\times10^{-1}\%, 1.05\%, 38.0\%$ and 100% , respectively.

Figure S6. Evolution of the V ($A_1 \sim G_1; x\%$) and H ($A_2 \sim G_2; x\%$) ($x = 1.00\times10^{-3}\%, 6.80\times10^{-3}\%, 1.25\times10^{-2}\%, 2.00\times10^{-2}\%, 1.00\times10^{-1}\%, 1.05\%$ and 38.0% , respectively) polarized fluorescence spectra of the FLU-HES/LDH ($x\%$) thin films with the following twist angles δ of the sample: (a) 60° , (b) 50° , (c) 40° , (d) 30° , (e) 20° , (f) 10° and (g) 0° . Spectra were recorded after excitation with vertical polarized light.

Figure S7. Evolution of the fluorescence dichroic ration of the FLU-HES/LDH ($x\%$) thin films with the emission wavelength for different twisting δ angles of the sample (see Figure S6 caption): (A)~(G) $x=1.00\times10^{-3}\%, 6.80\times10^{-3}\%, 1.25\times10^{-2}\%, 2.00\times10^{-2}\%, 1.00\times10^{-1}\%, 1.05\%$ and 38.0% , respectively. The linear relationship between the dichroic ration and $\cos^2(\delta+90)$ at 520 nm is included in inset graph.

Figure S8. A schematic representation for the orientation of FLU in the FLU-HES/LDH ($x\%$) materials: (A)~(G) $x=1.00\times10^{-3}\%, 6.80\times10^{-3}\%, 1.25\times10^{-2}\%, 2.00\times10^{-2}\%, 1.00\times10^{-1}\%, 1.05\%$ and 38.0% , respectively (Zn blue, C grey, H white, Al yellow, O red).

Figure S9. Cyclic voltammograms obtained with FLU-HES/LDH ($x\%$) thin film modified electrodes in 10^{-4} mol/L DA + 0.1 mol/L PBS (pH 7.0) at 100 mV/s.

Figure S10. The influence of pH value on CV behavior of FLU-HES/LDH ($x=1.25\times10^{-2}\%$) modified electrode in 10^{-4} mol/L DA + 0.1 mol/L PBS at 100 mV/s.

Figure S11. The stability of electrodes modified with different materials: (A) pristine FLU, (B) FLU/LDH physical mixture and (C) FLU-HES/LDH ($x=1.25\times10^{-2}\%$) in 10^{-5} mol/L DA + 0.1 mol/L PBS (pH 7.4) solution.

Figure S12. The stability of the FLU-HES/LDH ($x=1.25\times10^{-2}\%$) modified electrode in 10^{-5} mol/L DA + 0.1 mol/L PBS (pH 7.4) solution by recording cyclic voltammograms curves in consecutive 10 days measurement. a~j: from 1 to 10 days.

Figure S13. Cyclic voltammograms of the FLU-HES/LDH ($x=1.25\times10^{-2}\%$) modified electrode in 10^{-5} mol/L DA + 0.1 mol/L PBS (pH 7.4) solution at different scan rates (A) and the linear relationship between the anodic peak current and the scan rate (B).

Table S1: Chemical Compositions of the FLU-HES/LDH ($x\%$) Samples with Different FLU Content

Table S2: Fluorescence Decay Data of FLU in Solution and the FLU-HES/LDH ($x\%$) Samples

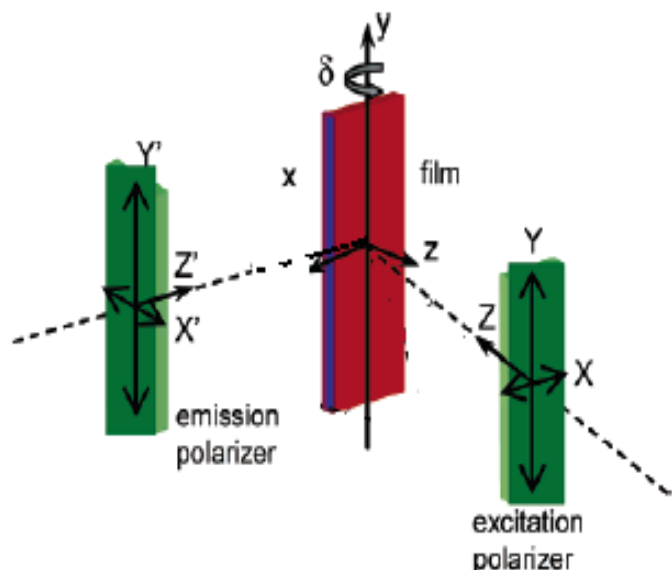


Figure S1. Three-dimensional perspective for the experimental setup to record fluorescence spectra with linear polarized light in the front-face configuration of a PTI Fluorescence instrument. The twist angle δ of the sample with respect to the excitation beam is also illustrated.

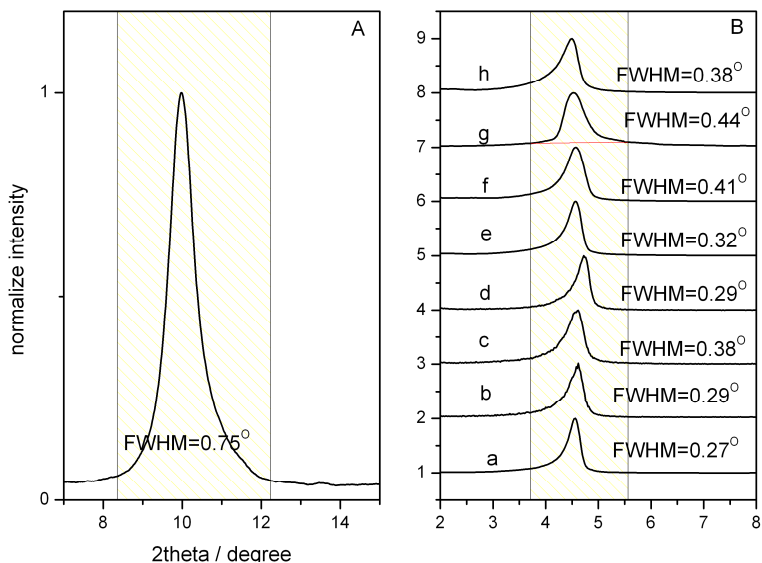


Figure S2. The FWHM of XRD patterns for (A) Zn₂Al-NO₃-LDH and (B) FLU-HES/LDH (x%): (a)~(h) $x=1.00\times10^{-3}\%$, $6.80\times10^{-3}\%$, $1.25\times10^{-2}\%$, $2.00\times10^{-2}\%$, $1.00\times10^{-1}\%$, 1.05%, 38.0% and 100%, respectively.

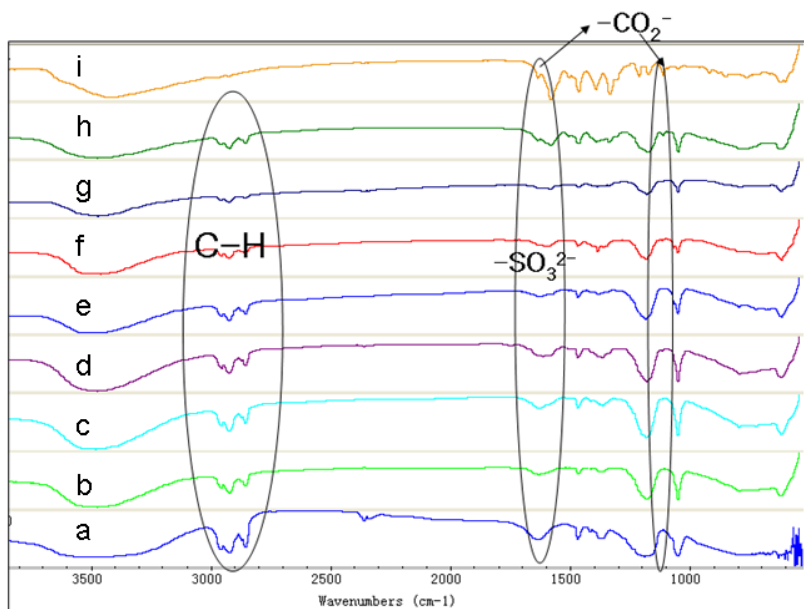


Figure S3. FT-IR spectra (4000~400 cm⁻¹ region) for the FLU-HES/LDH (x%): (a)~(i) $x=0$, $1.00\times10^{-3}\%$, $6.80\times10^{-3}\%$, $1.25\times10^{-2}\%$, $2.00\times10^{-2}\%$, $1.00\times10^{-1}\%$, 1.05%, 38.0% and 100%, respectively.

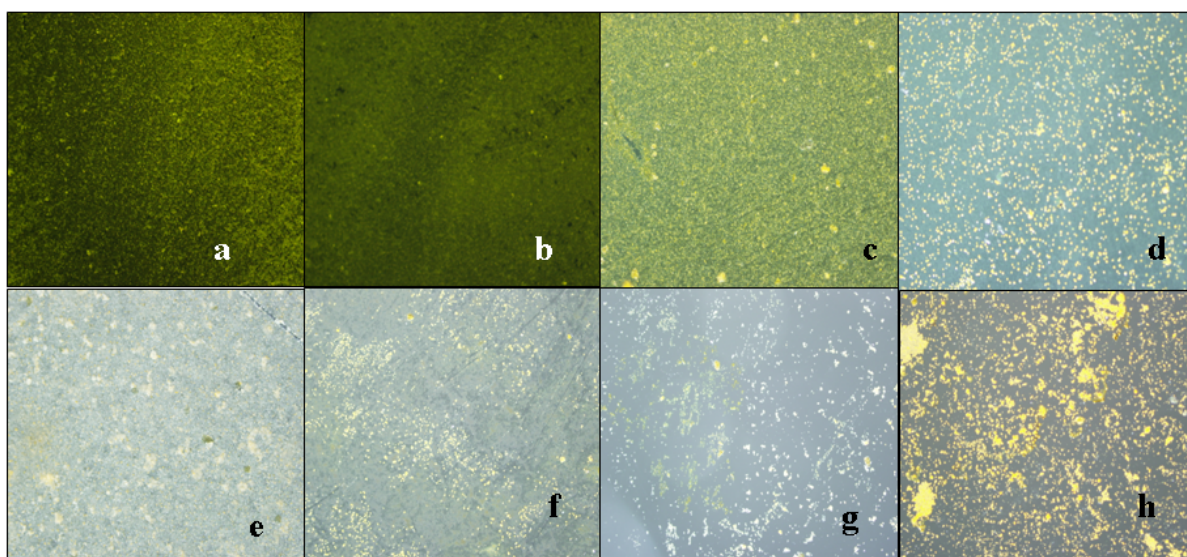


Figure S4. Fluorescent microscopic photographs of the FLU-HES/LDH films ($x\%$): (a)~(h) $x=1.00\times10^{-3}\%$, $6.80\times10^{-3}\%$, $1.25\times10^{-2}\%$, $2.00\times10^{-2}\%$, $1.00\times10^{-1}\%$, 1.05% , 38.0% and 100% . All the samples were excited by blue light.

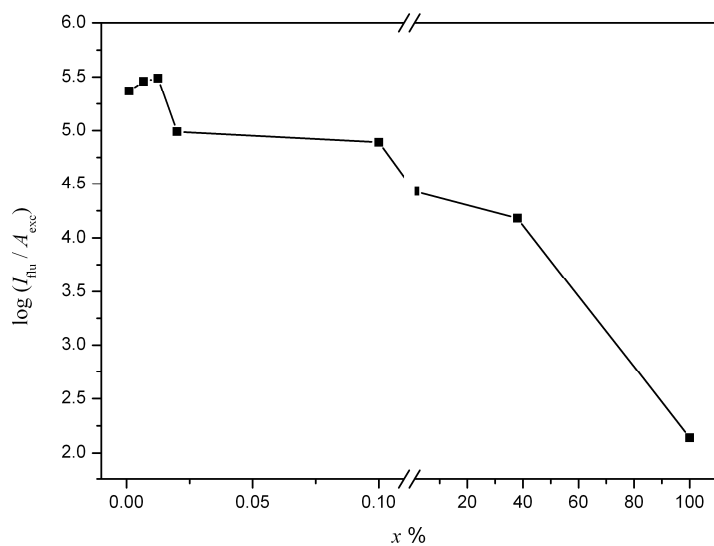


Figure S5. The fluorescence quantum yield varying with the increase of FLU content in the FLU-HES/LDH ($x\%$). $x=1.00\times10^{-3}\%$, $6.80\times10^{-3}\%$, $1.25\times10^{-2}\%$, $2.00\times10^{-2}\%$, $1.00\times10^{-1}\%$, 1.05% , 38.0% and 100% , respectively.

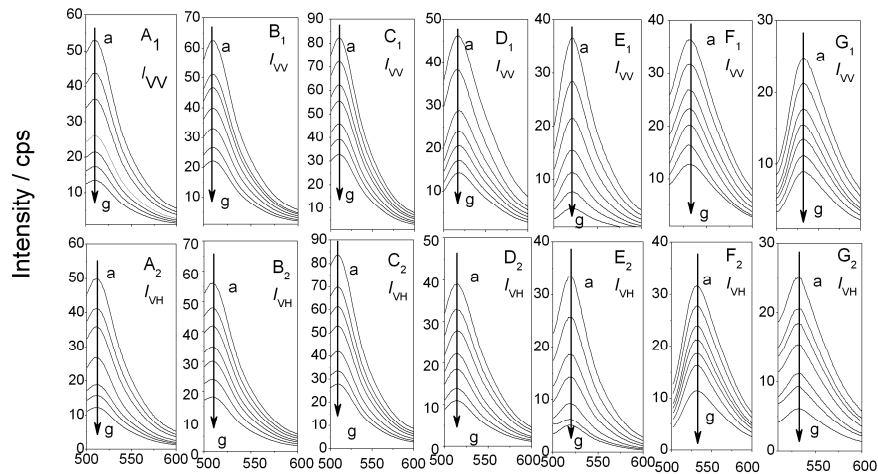


Figure S6. Evolution of the V ($A_1 \sim G_1$; $x\%$) and H ($A_2 \sim G_2$; $x\%$) ($x = 1.00 \times 10^{-3}\%$, $6.80 \times 10^{-3}\%$, $1.25 \times 10^{-2}\%$, $2.00 \times 10^{-2}\%$, $1.00 \times 10^{-1}\%$, 1.05% and 38.0% , respectively) polarized fluorescence spectra of the FLU-HES/LDH ($x\%$) thin films with the following twisting angles δ of the sample: (a) 60° , (b) 50° , (c) 40° , (d) 30° , (e) 20° , (f) 10° and (g) 0° . Spectra were recorded after excitation with vertical polarized light.

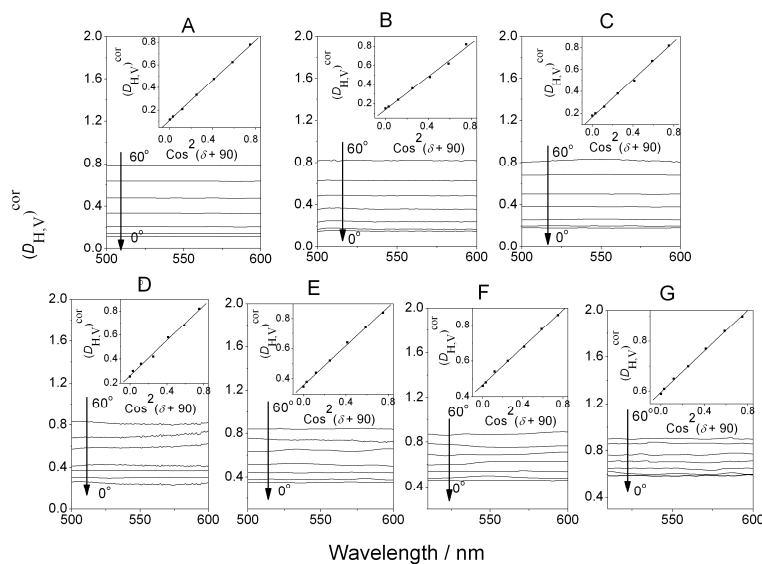


Figure S7. Evolution of the fluorescence dichroic ratio of the FLU-HES/LDH ($x\%$) thin films with the emission wavelength for different twisting δ angles of the sample (see Figure S6 caption): (A)~(G) $x = 1.00 \times 10^{-3}\%$, $6.80 \times 10^{-3}\%$, $1.25 \times 10^{-2}\%$, $2.00 \times 10^{-2}\%$, $1.00 \times 10^{-1}\%$, 1.05% and 38.0% , respectively. The linear relationship between the dichroic ration and $\cos^2(\delta+90)$ at 520 nm is included in inset graph.

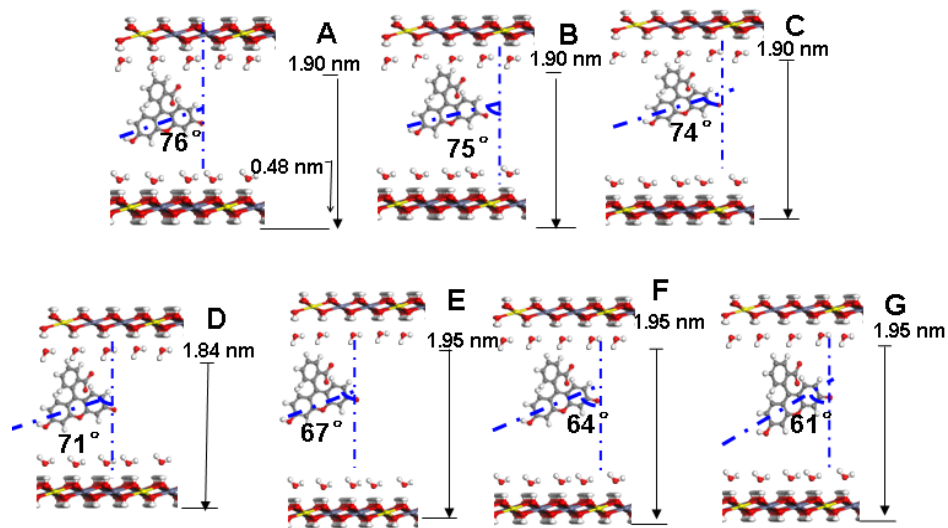


Figure S8. A schematic representation for the orientation of FLU in the FLU-HES/LDH ($x\%$) materials: (A)~(G) $x=1.00\times 10^{-3}\%$, $6.80\times 10^{-3}\%$, $1.25\times 10^{-2}\%$, $2.00\times 10^{-2}\%$, $1.00\times 10^{-1}\%$, 1.05% and 38.0% , respectively (Zn blue, C grey, H white, Al yellow, O red).

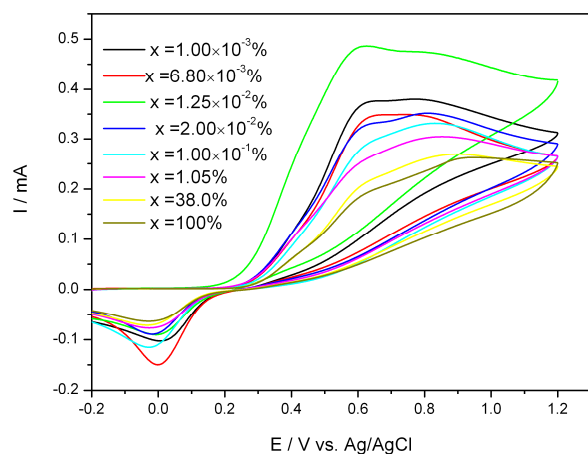


Figure S9. Cyclic voltammograms obtained with FLU-HES/LDH ($x\%$) thin film modified electrodes in 10^{-4} mol/L DA + 0.1 mol/L PBS (pH 7.0) at 100 mV/s.

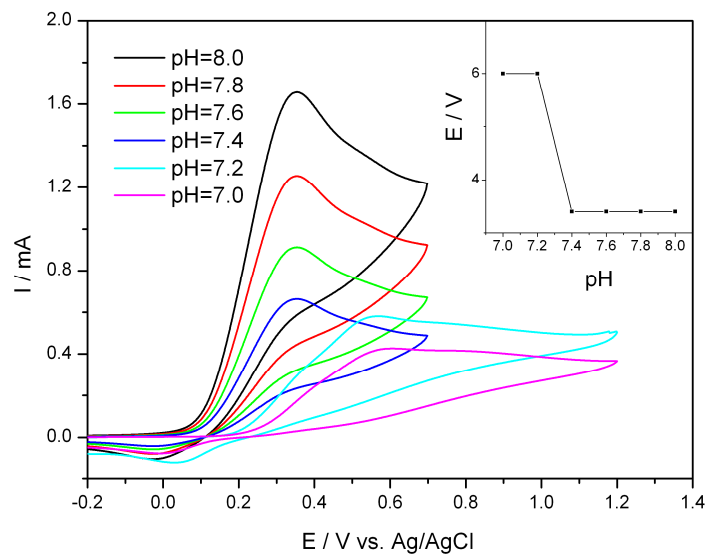


Figure S10. The influence of pH value on CV behavior of FLU-HES/LDH ($x=1.25\times 10^{-2}\%$) modified electrode in 10^{-4} mol/L DA + 0.1 mol/L PBS at 100 mV/s.

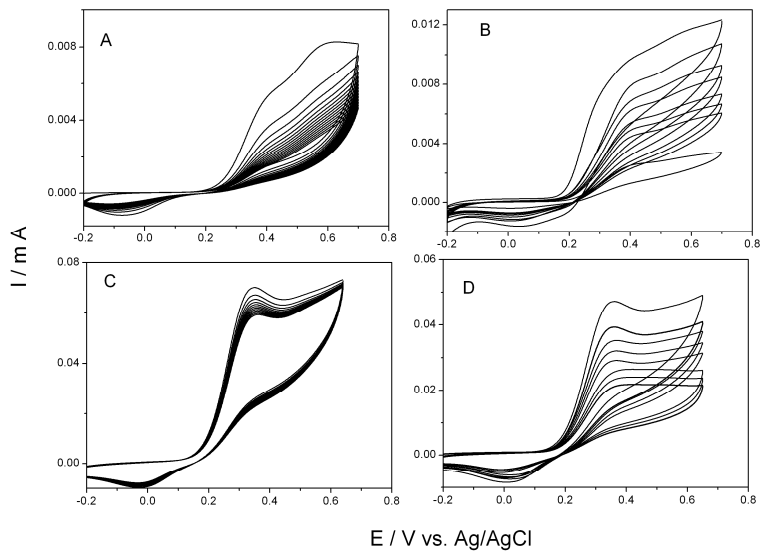


Figure S11. The stability of electrodes modified with different materials: (A) pristine FLU, (B) FLU/LDH physical mixture, (C) FLU-HES/LDH ($x=1.25\times 10^{-2}\%$) and (D) FLU-HES/LDH ($x=38.0\%$) in 10^{-5} mol/L DA + 0.1 mol/L PBS (pH 7.4) solution.

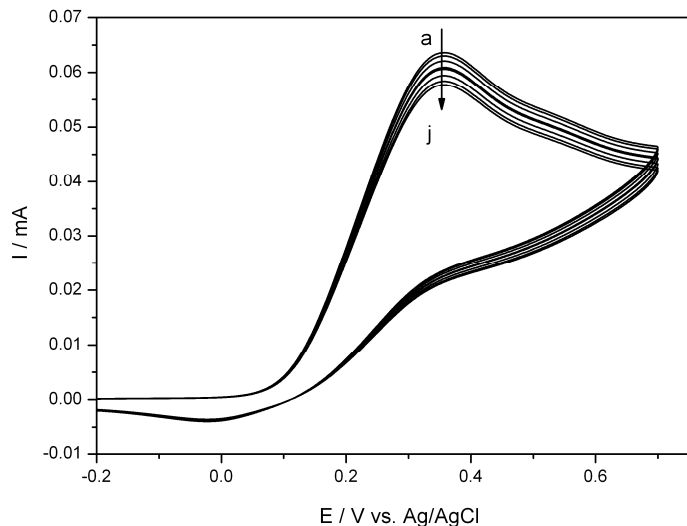


Figure S12. The stability of the FLU-HES/LDH ($x=1.25\times 10^{-2}\%$) modified electrode in 10^{-5} mol/L DA + 0.1 mol/L PBS (pH 7.4) solution by recording cyclic voltammograms curves in consecutive 10 days measurement. a~j: from 1 to 10 days.

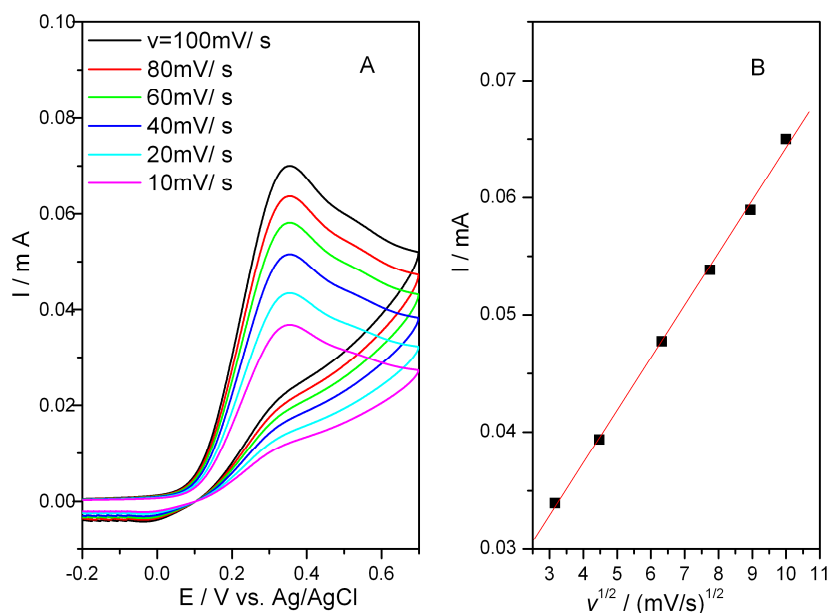


Figure S13. Cyclic voltammograms of the FLU-HES/LDH ($x=1.25\times 10^{-2}\%$) modified electrode in 10^{-5} mol/L DA + 0.1 mol/L PBS (pH 7.4) solution at different scan rates (A) and the linear relationship between the anodic peak current and the scan rate (B).

Table S1: Chemical Compositions of the FLU-HES/LDH ($x\%$) Samples with Different FLU Content

nominal content x (%)	chemical composition	Zn/Al ration	experimental content x (%)
0	[Zn _{0.68} Al _{0.32} (OH) ₂] (HES) _{0.32} · 1.59H ₂ O	2.13	0
1.34×10 ⁻³	[Zn _{0.67} Al _{0.33} (OH) ₂](FLU) _{X1} (HES) _{Y1} · 0.49H ₂ O	2.03	1.00×10 ⁻³
8.00×10 ⁻³	[Zn _{0.68} Al _{0.32} (OH) ₂](FLU) _{X2} (HES) _{Y2} · 1.06H ₂ O	2.13	6.80×10 ⁻³
1.34×10 ⁻²	[Zn _{0.66} Al _{0.34} (OH) ₂](FLU) _{X3} (HES) _{Y3} · 0.88H ₂ O	1.94	1.25×10 ⁻²
2.35×10 ⁻²	[Zn _{0.69} Al _{0.31} (OH) ₂](FLU) _{X4} (HES) _{Y4} · 0.33H ₂ O	2.22	2.00×10 ⁻²
1.18×10 ⁻¹	[Zn _{0.67} Al _{0.33} (OH) ₂](FLU) _{X5} (HES) _{Y5} · 0.37H ₂ O	2.03	1.00×10 ⁻¹
1.16	[Zn _{0.68} Al _{0.32} (OH) ₂](FLU) _{X6} (HES) _{Y6} · 0.92H ₂ O	2.13	1.05
41.0	[Zn _{0.68} Al _{0.32} (OH) ₂](FLU) _{X7} (HES) _{Y7} · 0.92H ₂ O	2.13	38.0
100	[Zn _{0.67} Al _{0.34} (OH) ₂] (FLU) _{0.34} · 1.31H ₂ O	1.97	100

$X_1=3.30\times10^{-6}$, $Y_1=0.329$; $X_2=2.17\times10^{-5}$, $Y_2=0.319$; $X_3=4.25\times10^{-5}$, $Y_3=0.339$; $X_4=6.21\times10^{-5}$, $Y_4=0.309$;
 $X_5=3.00\times10^{-4}$, $Y_5=0.329$; $X_6=3.40\times10^{-3}$, $Y_6=0.316$; $X_7=0.122$, $Y_7=0.198$.

Table S2: Fluorescence Decay Data of FLU in Solution and the FLU-HES/LDH ($x\%$) Samples

x (%)	n	τ_i (ns)	A_i (%)	$\langle\tau\rangle$ (ns)	Chi^2
1.00×10 ⁻³	2	3.32	38.1	1.97	1.23
		1.15	61.9		
6.80×10 ⁻³	2	4.82	48.2	2.87	1.34
		1.57	51.8		
1.25×10 ⁻²	2	4.36	54.8	3.46	1.49
		2.37	45.2		
2.00×10 ⁻²	2	4.83	56.5	3.76	1.19
		1.94	43.5		
1.00×10 ⁻¹	2	0.29	31.5	1.90	1.80
		2.63	68.5		
1.05	2	0.27	41.7	1.81	1.34
		2.89	58.3		
38.0	2	0.1	53.4	1.43	1.65
		3.0	46.6		
100	2	0.09	65.9	0.12	1.97
		0.17	35.1		
solution/10 ⁻⁵ mol/L	1	1.80	100	1.80	1.22

τ is the fluorescence lifetime; $\langle\tau\rangle$ is the intensity average lifetime. The goodness of fit is indicated by the value of Chi^2 .